RSC Advances

ROYAL SOCIETY OF CHEMISTRY

www.rsc.org/advances

Graphical Abstract

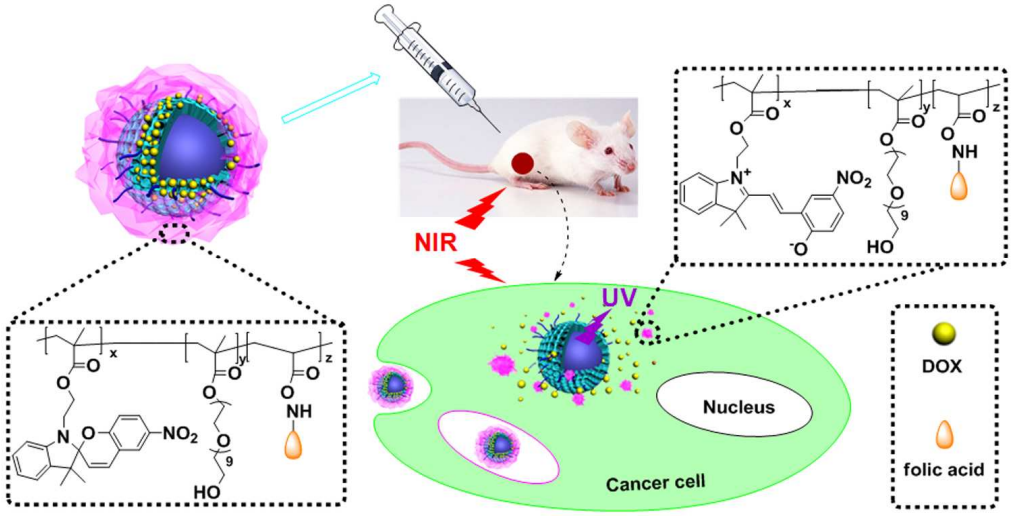

The core-shell nanocarrier based on spiropyran-containing copolymer coated upconversion nanocompsites was successfully prepared via a facile self-assembly process for NIR-triggered drug release and cancer therapy. In this strategy, the loaded drug could be released *via* NIR (λ= 980 nm) irradiation after the nanocarrier was endocytosed by cancer cells. And the sustained release of anticancer drug could inhibted the growth of tumor effectively.

Cite this: DOI: 10.1039/c0xx00000x

www.rsc.org/xxxxxx

ARTICLE TYPE

Near-Infrared light-controlled drug release and cancer therapy with polymer-caged upconversion nanoparticles

Qingjian Xing [a], Najun Li*[a,c], Yang Jiao[b], Dongyun Chen [a], Jiaying Xu[b], Qingfeng Xu[a,c] and Jianmei Lu*[a,c]

Received (in XXX, XXX) Xth XXXXXXXXX 20XX, Accepted Xth XXXXXXXXX 20XX

DOI: 10.1039/b000000x

Herein, a core-shell nanocomposite was fabricated by self-assembly of the photo-responsive copolymers with silica-coated upconversion nanoparticles for near-infrared light-controlled drug release and cancer therapy. Firstly, lanthanide upconversion nanoparticles (UCNPs) co-doped with Yb^{3+} and Tm^{3+} were encapsulated with mesoporous silica as the core (MUCNPs). Then a folate conjugated light-responsive copolymer (PSMN-FA) was synthesized and coated on MUCNP as shell via self-assembly. Anti-cancer drugs could be loaded in the mesopores of silica layer before polymer coating. Upon the near-infrared (NIR) light irradiation at 980 nm, the caged UCNPs emitted luminescence at UV region, which could change the structure of amphiphilic copolymer and separate from MUCNPs, immediately following the release of the pre-loaded drugs after targeted in cancer cells. Our model experiments *in vitro* verified that the nanocarrier MUCNPs@C18@PSMN-FAcan provide active tumor targeting to folate receptor over-expressed (FR+) tumor cells. Both *vitro* and *vivo* studies were carried out to evaluate the NIR-controlled drug release strategy and the promising application in anticancer therapy based on the polymer-UCNPs nanocomposites.

Introduction

Multifunctional drug delivery systems based on smart copolymer have become a major intense research for their various potential applications in biomedical field.[1] Generally, the copolymer were designed to respond to external stimuli (e.g. pH, temperature, redox, light, enzymes) and used in controlled drug delivery systems.[2] Compared with other stimuli, light was considered as an ideal external trigger because it could be used without the limit of time and space and was harmless if applied correctly.[3]Therefore, a large amount of copolymers containing light-responsive groups, such as azobenzene, spiropyran, *o*-nitrobenzyl and coumarin, have been designed and applied in polymeric micelles drug release systems.[4] The polymeric micelles could load anticancer drugs via a self-assembly process and release them upon light exposure. Since the light trigger could be switched between "on" and "off", it was easy to control the drug release, which was an advantage compared with other stimuli-responsive drug release systems.[5]

Typically, most copolymers containing photo-responsive groups were sensitive and degradable upon UV light.[6] However, the disadvantages of UV light, its high energy and short penetration depth, could not be ignored for the limitation in biomedical applications.[7] Near-infrared (NIR) light, a stimulus used *in vivo* for minimally invasive therapy, has drawn more and more interest in light-responsive polymeric drug delivery systems for its low energy and ability to penetrate deeply into tissues.[8] Lanthanide upconversion nanoparticles (UCNPs) could convert continuous-wave NIR light into different wavelengths of light in UV and visible regions. Especially, UCNPs co-doped with Yb^{3+} and Tm^{3+}were capable of converting NIR light into high-energy UV emission.[9] Therefore, the former UV light-responsive copolymers could be utilized with caged UCNPs for potential biomedical applications under the irradiation of low-energy NIR light, which could avoid the damage of tissues from UV light. Besides, like the other functional nanoparticels used in bioimaging, the UCNPs was also confirmed to be applied in high sensitive bioimaging due to its high photochemical stability and improved tissue penetration depth.[10]

Herein, lanthanide UCNPs co-doped with Yb^{3+} and Tm^{3+} were introduced into the nanocarrier with the photo-responsive polymeric shell containing spiropyran groups which is utilized as the photo trigger in our previous work.[11] With the cooperation of the caged UCNPs, the drug release of the nanocomposite could be controlled by NIR light directly as well as the bioimaging based on upconversion luminescence (UCL). The core-shell nanocomposite was assembled by spiropyran-containing copolymers and silica-coated UCNPs (Scheme 1). In order to target to over-expressed folate receptor (FR+)tumor cells, the spiropyran-containing copolymer was conjugated with folic acid to obtain PSMN-FA. On the other hand, lanthanide UCNPs co-doped with Yb^{3+} and Tm^{3+} were synthesized and then caged by mesoporous silica layer (MUCNPs) for drug loading. After modified with hydrophobic long alkyl chains (C18), MUCNPs were coated by the amphiphilic polymer PSMN-FA through hydrophobic van der Waals interaction via a self-assembly process to obtain the nanocarrier MUCNP@C18@PSMN-FA. The NIR light-controlled drug release and cancer targeting as well as antitumor effect were investigated in *vitro* and in *vivo*.

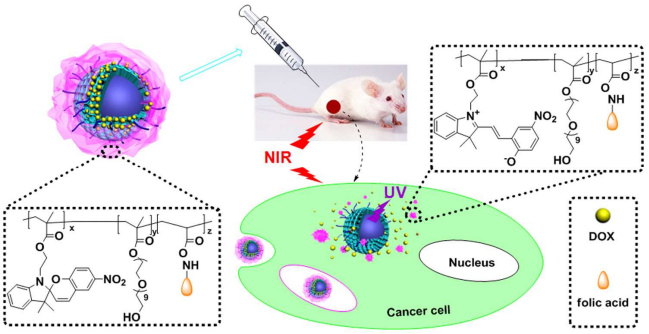

Scheme 1 Schematic illustration of upconversion nanoparticles/polymer multifunctional nanocomposite and the NIR light-trigged drug release process.

Experimental Section

Materials

2, 3, 3-trimethyl-3H-indol, 2-hydroxy-5-nitrobenzaldehyde and 2-bromoethanol were purchased from TCI. Poly (ethylene glycol) methacrylate (MAPEG, Mn average= 526), $Y(CH_3CO_2)_3$, $Yb(CH_3CO_2)_3$, $Tm(CH_3CO_2)_3$, octadecene and oleic acid were purchased from Aldrich. All the other regents were purchased from Aladdin Reagent.

Synthesis of silica-modified UCNPs (MUCNPs)

The UCNPs were synthesized according to the literature.[12] The silica shell was coated via the surfactant-assistant sol-gel coating method according to the literature with little modification.[13] Generally, 100 mg UCNPs were added to 20 mL of Triton X-100 solution and 80 mL DI water was added before the solution was treated with sonication for 10 min. The solution was allowed to stir for 6 h and the nanoparticles were collected after centrifugation. The UCNPs were washed with water and then disperse into a mixture of ethanol (160 mL), DI water (40 mL) and 2 mL of 28 wt% ammonia aqueous solution. The mixture was stirred for 30 min and then 0.06 g of TEOS was added. After 6 h, the product was collected by centrifugation and then washed with ethanol and water. The nanoparticles were redispersed into a mixed solution containing 300 mg CTAB, 80 mL DI water, 60 mL ethanol and 1 mL ammonia aqueous solution. After treated with sonication for 30 min, the solution was stirred vigorously while 0.30 g TEOS was added by dropwise. After 6 h, the core-shell nanoparticles were collected by centrifugation and washed with ethanol and water for several times. Finally, the nanoparticles were redispersed in 80 mL ethanol and the mixture was refluxed over night to remove the CTAB. The product was collected by centrifugation and washed with ethanol for three times before dried under vacuum.

Synthesis of light-responsive copolymer Poly (SPMA-MAPEG-NAS) (PSMN)

The light-responsive amphiphilic copolymer poly (SPMA-MAPEG-NSA) (PSMN) was prepared by free radical copolymerization of SPMA, NAS and MAPEG in cyclohexanone using AIBN initiator. Typically, AIBN (1.0 mg) was added to a cyclohexanone solution (2 mL) with SPMA (84 mg, 0.2 mmol), MAPEG (315 mg, 0.6 mmol) and NAS (8.5 mg, 0.05mmol) in a test tube. The test tube was sealed and cycled between vacuum and nitrogen thrice. After 7 h reaction in an oil bath at 70 °C, the mixture was concentrated in a rotary evaporator and washed with a large quantity of anhydrous ether. The precipitate was recovered by centrifugation, dried under vacuum and stored in a desiccator for further use.

Synthesis of folate conjugated copolymer PSMN-FA

The conjugation procedure was briefly as follows. Folic acid (30 mg) was added to dry pyridine containing 200 mg of the above copolymer. The solution was stirred for 12 h at room temperature against visible light exposure. Then, the mixture was precipitated in 10 % acetone in anhydrous ether. The copolymer PSMN-FA was obtained by centrifugation and stored in the dark at 4 °C.

Preparation of the core-shell nanocarrier (MUCNPs@C18@PSMN-FA)

Firstly, the MUCNPs were modified with long alkyl chain (MUCNP@C18) to improve the hydrophobicity of the surface using a facile method utilized in our previous work.[11] After that, MUCNP@C18 (5 mg) was dispersed in 1 mL tetrahydrofuran by sonication for 5 min. PSMN-FA (30 mg) was dissolved in the solution afterward. Then, 5 mL distilled water was added dropwise to the above solution with vigorous stirring and the resulting mixture was stirred vigorously over night to evaporate the tetrahydrofuran. After that, the product was separated by centrifugation and washed with distilled water several times.

Drug loading and release experiment

To evaluate the drug loading and release properties, doxorubicin (DOX) was used as a model anticancer agent. DOX was extracted from doxorubicin hydrochloride (DOX·HCl) according to the procedure reported previously.[14] MUCNP@C18 (10, 5 and 1 mg) was first dispersed into 1 mL phosphate buffered saline (PBS) solution and the mixture was treated with ultrasonic for 15 min. After that, then DOX solution (5 mg·ml^{-1}, 100 μL) was added and he mixture was stirred vigorously for 24 h against visible light exposure. After that, DOX-MUCNP@C18 were obtained by centrifugation (5000 rpm, 5min) and washed with PBS for several times, then dried at 60 °C under vacuum for further usage.

To evaluate the amount of drug loaded by MUCNP@C18, UV-Vis spectroscopy was used for analysis. First, the calibration curve of DOX was determined by taking absorbance *vs.* DOX concentration between 0 and 5 mg L^{-1} as parameters, and the calibration curve was fitted to the Lambert-Beer law as follows:

$$A=0.0014+0.0091C$$

Where A is the absorbance and C is the concentration (mg L^{-1}). After adsorption, the DOX solution (100 μL) was extracted and diluted to 10 mL, and then analyzed by UV-Vis spectroscopy at a wavelength of 485 nm. Drug loading content and drug loading efficiency can be calculated as follows:

Drug loading content (wt %) = (weight of loaded drug/weight of nanocarrier) × 100%

Drug loading efficiency (%) = (weight of loading drug/weight of drug in feed) × 100%

Light-triggered release of DOX in was done by mixing 5 mg DOX-MUCNP@C18@PSMN-FA with 5 mL PBS buffer solution and the solution was irradiated with a 980 nm NIR laser for different time duration at a certain power density. The control experiment was done without any NIR irradiation.

Cell culture and preparation

Human KB cell lines with folic acid receptor (FR(+)), A549 human alveolar adenocarcinoma cell lines without folic acid receptor (FR(-)) and Human bronchial epithelial cells (Beas2B) were purchased from Shanghai Cell Institute Country Cell Bank, China and cultured as monolayers in RPMI-1640 medium supplemented with 10% heat-inactivated fatal bovine serum at 37 ^{o}C in a humidified incubator (5% CO_2 in air, v/v).

Light-triggered DOX release in KB cells and the Cell cytotoxicity assay

KB cells were seeded in a 96-well plate at a density of 1.3×10^4 cells per well and cultured in 5 % CO_2 at 37 ^{o}C for 24 h. Then, different materials were added to the medium. For materials without NIR irradiation, the cells were incubated in 5 % CO_2 at 37 ^{o}C for varied time. For materials with NIR irradiation, the nanocarriers were removed after 3 h of incubation, followed by exposing to different NIR dosage. In *vitro* cytotoxicity was assessed by the MTT assay. The cells were further incubated for another 24 h in the dark. After that, the medium was removed and 100 μL of MTT solution was added and incubated for another 3 h. The medium was replaced with 100 μL of DMSO and the absorbance was monitored using a microplate reader at the wavelength of 485 nm. The cytotoxicity was expressed as the percentage of cell viability compared to untreated control cells.

CLSM observation of the cell uptake

For CLSM observation of the cell uptake, A549 cells and KB cells were seeded in cover glass bottom dishes and then treated with nanocarrier MUCNP@C18@PSMN-FA at a concentration of 200 μg/ mL. After 2 h of incubation, the media was removed and the cells were washed twice with D-Hank's solution to remove the residual nanocarriers. After that, 500 μL of DAPI solution in PBS (10 %) was added and incubated for another 20 min to stain the nuclei and fix the cells. After the incubation, the cells were washed with excessive DAPI and 1 mL of D-Hank's solution was added at last. The cells were visualized under a confocal laser scanning microscope (Olympus, FV 1000).

In *vivo* systematic toxicity

To evaluate the safety of DOX-MUCNP@C18@PSMN-FA in vivo, the normal nude mice without tumors were randomly divided into three groups (four mice per group): saline, DOX-loaded nanocarrier without or with laser treatment. 24 hours after intraperitoneal injection, the mice without laser treatment were sacrificed, and organs including heart, liver, spleen, lung and kidney were harvested for histopathological examination with Haematoxylin & Eosin (H&E) staining. And at the end of treatment process (19 d), the groups of saline and DOX-loaded nanocarrier with laser treatment were treated with the same histopathological examination.

In *vivo* antitumor effect studies

All animal experiments were performed under protocols approved by Soochow University Laboratory Animal Center. Folate receptor positive (FR +) KB cells (1×10^6) were implanted in the right back area of 4 weeks old nude mice subcutaneously. Tumor volume was calculated by the following equation: Volume= $0.5 \times a \times b^2$, where (a) and (b) represent the width and length of the tumor. For comparative purpose, the tumor volume was normalized by its initial volume as V/V_0 (V_0 was the volume of the tumor when the treatment was started). The nude mice were divided into two groups (n=4). DOX-MUCNP@C18@PSMN-FA in 100 μL 0.9 % NaCl solution was injected via intratumoral injection at an interval of 2 days at a dosage of 5 mg DOX/Kg body weight. And the same volumes of 0.9 % NaCl solution was injected into control groups. After DOX loaded nanocarriers were injected into the tumor, the nude mice were treated with NIR irradiation (60 mW cm^{-2}).

Characterization

^{1}H NMR spectra were measured by an INOVA 400MHz NMR instrument. FTIR measurements were performed as KBr pellets on a Nicolet 4700 spectrometer (Thermo Fisher Scientific) in the range of 400-4000 cm^{-1}. The UV-Vis absorption spectra were measured on a TU-1901 spectrophotometer. Fluorescence spectra were measured on a HORIBA JobinYvon's fluorescence spectrofluorometers. Gel permeation chromatography (GPC) analysis was carried out on a Waters 1515 pump and a differential refractometer, THF was used as a mobile phase at a flow rate of 1.0 mL/min. TEM images were obtained using a TecnaiG220 electron microscope at an acceleration voltage of 200 kV. Brunauer-Emmett-Teller (BET) and Barrett-Joyner-Halenda (BJH) analyses were used to determine the surface area, pore size and pore volume and measurements were obtained with a Quantachrome Autosorb 1C apparatus at -196 ^{o}C under continuous adsorption conditions. Energy dispersive spectrometry (EDS) was taken on a Hitachi S-4700 equipped with an energy-dispersive X-ray spectrometer. Confocal laser scanning microscopy (CLSM) images were observed by a confocal laser scanning microscopy (Olympus, FV 1000). Continuous wave 980 nm NIR laser (0-12 W adjustable, Hi-tech Optoelectronics Co., Ltd.) was used for irradiation.

Results and Discussion

Fabrication of the core-shell nanocarrier MUCNPs@C18@PSMN-FA

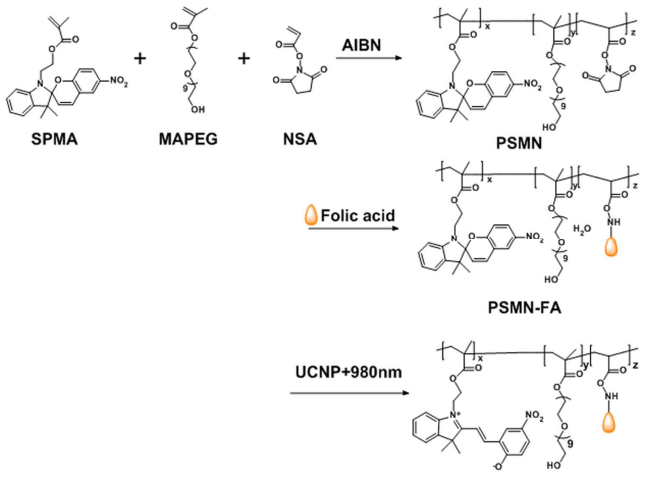

Scheme 2 The synthetic route of amphiphilic light-responsive copolymer PSMN-FA.

The amphiphilic light-responsive copolymer PSMN-FA was synthesized following the procedure shown in Scheme 2. The

GPC data of the copolymer with different molar ratios were summarized in Table S1. PSMN (M_n=24100, PDI=1.52) was chosen to be conjugated with FA-NHS to obtain PSMN-FA (M_n=27800, PDI=1.72). And there was about 13.3 wt% folic acid on average were conjugated with PSMN according to the incremental quantity of the molecular weight. The structure of PSMN and PSMN-FA was confirmed by ^{1}H NMR, from which the characteristic peaks in SPMA (δ=6.88, 7.16 and 8.03 ppm), NAS (δ=2.84 ppm) and folic acid (δ=4.54, 4.70 and 8.20 ppm) were all observed correspondingly, confirming that the amphiphilic copolymer PSMN-FA were synthesized successfully.

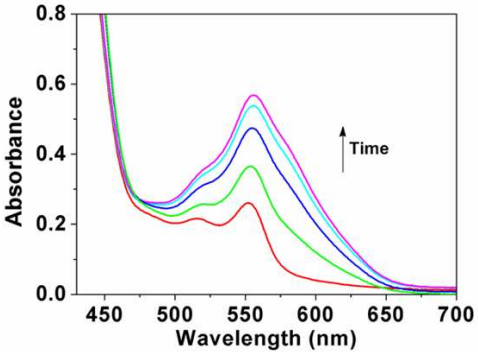

Fig. 1 The absorbance of PSMN after UV irradiation.

Spiropyran can be reversibly switched between the non-colored closed-loop state (SP, spiroform) and another colored open-loop state (MC, merocyanineform) by irradiation with visible light and ultraviolet light. The UV-Vis absorption of PSMN-FA after irradiation with UV light was showed in Fig. 1. With the increasing of the time of UV irradiation, the absorbance at 550 nm had an obvious increase which ascribed to the conversion of SP to MC.

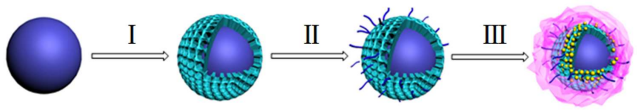

Scheme 3 Synthetic route to MUCNP@C18@PSMN-FA: I) TEOS and CTAB;II) C18;III) DOX loading and self-assembly.

The β-$NaYF_4$:Tm^{3+} 0.5 mol%, Yb^{3+} 30 mol% / β-$NaYF_4$ nanoparticles (UCNPs) were utilized as optical core and the mesoporous silica shell acted as DOX carrier. After modified with long alkyl chain (C18), the surface of MUCNP turned to be hydrophobic. And the amphiphilic copolymer PSMN-FA could coat on the surface through hydrophobic van der Waals interactions via a self-assembly process (Scheme 3).

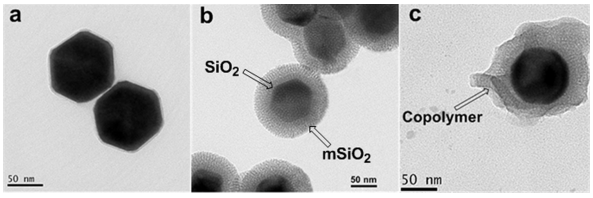

Fig. 2 TEM images of UCNP (a), MUCNP (b) and MUCNP@C18@PSMN-FA (c).

The detailed morphological features of the nanoparticles before and after modification were determined by TEM. After modified via the surfactant-assistant sol-gel coating method, the UCNPs were coated with a thin normal silica layer and a thicker mesoporous silica layer (Fig. 2b). The DLS result (Fig. S1) showed that MUCNP@C18nanoparticles gained an average diameter of 145 nm after modification which corresponded to the results of TEM measurement. The amphiphilic copolymers were coated onto the hydrophobic surface of MUCNP@C18 nanoparticles through a self-assembly process via van der Waals interactions. After the self-assembly, the profile of nanocarrier became blurred and a thick layer of copolymer film was clearly observed (Fig. 2c). All the results confirmed that the core-shell nanocarrier was synthesized successfully.

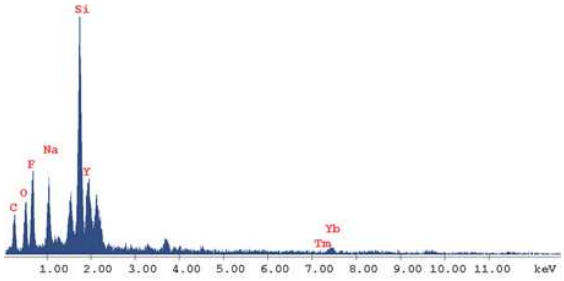

Fig. 3 EDS analyses of the MUCNP nanoparticles.

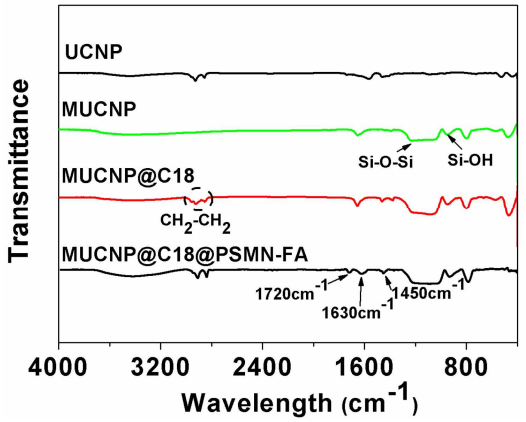

Fig. 4 FTIR spectra of UCNP, MUCNP, MUCNP@C18 and MUCNP@C18@PSMN-FA.

Energy dispersive spectrometry (EDS) and Fourier transform infrared (FTIR) spectra also provided evidence for the modification process of the core-shell nanocarrier. As shown in Fig. 3, a strong peak of silica could be observed which confirmed that the UCNPs were coated with silica layer successfully. And the FTIR measurement provided the same results that the peaks at 802, 947 and 1083 cm^{-1} belong to Si-OH and Si-O-Si were observed obviously. The surface of MUCNP was enriched with Si-OH which could be easily modified with C18. And the peak at 2890 cm^{-1} belong to C-H_x could provide that expectation (Fig. 4). All the results above confirmed a success formation of MUCNP@C18. The N_2 adsorption/desorption isotherms of MUCNP@C18 (Fig. S2) indicated that the modification of C18 did not affect the pore structure of MUCNP, which is significant for drug loading and release. And in the spectrum of MUCNP@C18@PSMN-FA, the appearance of IR peaks at 1720, 1630 and 1450 cm^{-1} should be attributed to the C=O, N-H and C-H bending of benzene ring respectively which indicated the copolymer were coated on the nanocore successfully.

The fluorescence spectra were taken to measure the optical

performance of the nanocarrier. Upon irradiation at 980 nm (power intensity= 12 W), the luminescence emanates from the excited UCNPs located at the UV region as blue light (insert photographs of Fig. 5). The luminescence intensity of MUCNP@C18@PSMN-FA, especially below 400 nm, was obviously lower when comparing with the spectrum of free MUCNP@C18 in solution (Fig. 5). This was no surprise because the light-responsive copolymer absorbed most of the light (λ= 365 nm) emitted by the UCNPs core.

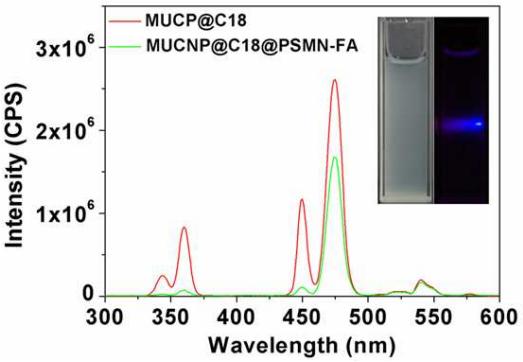

Fig. 5 The emission spectra of MUCNP@C18 and MUCNP@C18@PSMN-FA (the insert optical photographs showed the light emission of MUCNP@C18 nanoparticles upon 980 nm laser exposure).

Drug loading and release

DOX was chosen as model anti-cancer drug to discuss the drug loading and release behaviour of MUCNP@C18@PSMN-FA. The actual loading efficiency of DOX in the nanocarrier was determined by the characteristic DOX absorbance at 485 nm (Table S2). In our strategy, the amphiphilic copolymer could undergo structural transformation upon MUCNP-excited UV light irradiation, resulting in the copolymer to shift the hydrophilic-hydrophobic balance to be a hydrophilic one. Since the surface of hydrocarbon octadecyltrimethoxysilane (C18) modified MUCNP was hydrophobic, the hydrophilic copolymer would detach from the MUCNP, triggering the release of drugs loaded in the mesoporous silica channels. And the results of DOX release from the MUCNP@C18@PSMN-FA nanocarrier were shown in Fig. 6. Previously, DOX loaded nanocarrier was immersed in PBS buffer at 37 °C. When the nanocarrier received no NIR exposure, there was a very small amount of DOX (less than 5 wt %) was released. However, an obvious release amount of DOX was measured when the nanocarrier was irradiated with NIR laser at 980 nm. The DOX release amount controlled by NIR light reached 50 wt % in 6 h and another about 30 wt % of DOX could be released continuously in 28 h. Compared to the control experiment without NIR light irradiation, the obvious release of DOX upon NIR light irradiation confirmed our NIR light triggered drug release strategy. Moreover, the drug release was obviously dependent on the on-off pattern of the excited source which indicated that the drug release could be tuned by remote control of the NIR laser irradiation (Fig. 6b). And the slight rise of DOX concentration after the switching off the NIR irradiation could be attributed to the relatively slow transfer of DOX from MUCNPs into the PBS solution.

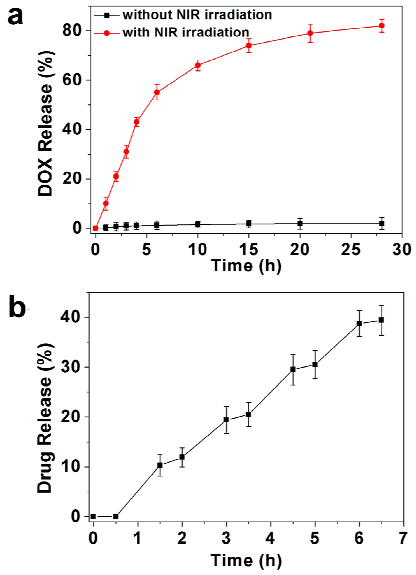

Fig. 6 (a) Release profile of DOX from MUCNP@C18@PSMN-FA nanocarrier in PBS buffer with or without NIR (980 nm) irradiation at power density of 12 W. (b) Drug release in PBS under NIR light irradiation and dark conditions, alternatively.

Light-triggered DOX release in KB cells and the Cell cytotoxicity assay

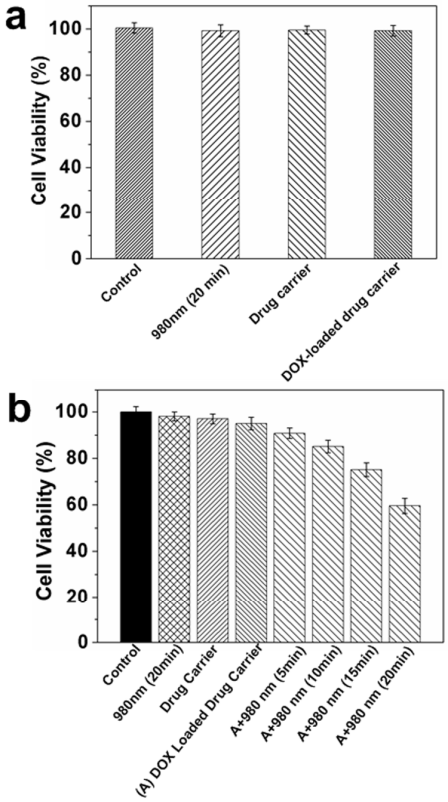

Fig. 7 (a) Incubation of normal Beas2B cell growth in the presence of excitation at 980 nm (20 min), drug carrier (MUCNP@C18@PSMN-FA) and DOX- loaded drug carrier (DOX-MUCNP@C18@PSMN-FA) without NIR light exposure. (b)Incubation of KB cell growth in the presence of excitation at 980 nm, drug carrier and DOX loaded drug carrier without or with NIR light exposure for varied dosages after 24 h of incubation. The concentration of drug carrier was 0.5 mg/mL, and the NIR light power intensity was 3 W/cm^2.

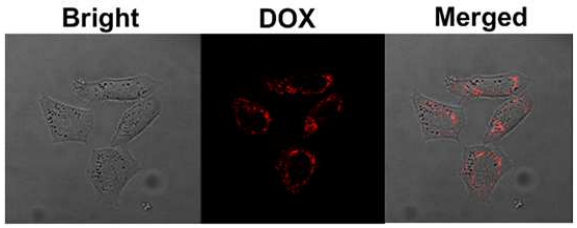

Fig. 8 CLSM observation of DOX release.

The controlled DOX release studied were carried out by incubating with KB cells to confirm the feasibility of using this system. Prior to the drug release experiment in *vitro*, we incubated KB and normal Beas2B cells in the culture medium with NIR exposure, MUCNP@C18@PSMN-FA and DOX-MUCNP@C18@PSMN-FA as the controls. The in *vitro* cytotoxicity of DOX-MUCNP@C18@PSMN-FA upon NIR irradiation was evaluated by the MTT assay. After treated with varied dosages of NIR exposure, the KB cells were incubated for another 3 h. Then, the nanocarriers were removed and the cells were incubated for further 24 h in the dark. All the results were summarized in Fig. 7. Treatments with NIR light, MUCNP@C18@PSMN-FA loaded with and without DOX did not result in an obvious decrease in cell viability, suggesting no harm of NIR light and our drug carrier was biocompatible to the normal cells (Fig. 7a). On the contrary, a significant decrease of cell viability was observed when the DOX loaded drug carrier was treated with NIR light, indicating the effective delivery of DOX into the tumor cells (Fig. 7b). And the CLSM images of KB cells upon NIR light irradiation could also confirm the drug release (Fig. 8).

CLSM observation of the cell uptake

To investigate the properties of MUCNP@C18@PSMN-FA nanocarrier in tumor cell targeting and cell imaging, the cellular uptake of nanocarriers for FR(+) and FR(-) cells was performed. The confocal laser scanning microscopy (CLSM) images of cells with MUCNP@C18@PSMN-FA solution after the same incubation time are shown in Fig. 9. After excited with 980 nm NIR light, the emission light of UCNPs could be observed and the intensity of the fluorescence was used to judge the cell uptake of nanocarrier. And a stronger fluorescence could be observed obviously in KB cells by comparison of A549 cells. The significant difference of fluorescence intensity suggested the targeting moiety offered by folic acid is efficient at enhancing tumor cell targeting in *vitro*.

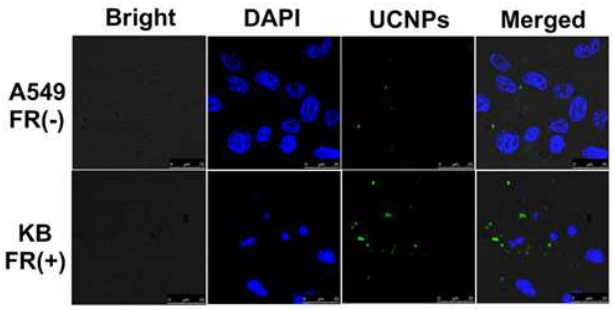

Fig. 9 CLSM observation of FR (-) A549 cells and FR (+) KB cells incubated with MUCNP@C18@PSMN-FA (200 μg/mL) for 2 h.

Evaluation of antitumor effect of NIR-triggered DOX release in *vivo* and the systematic toxicity

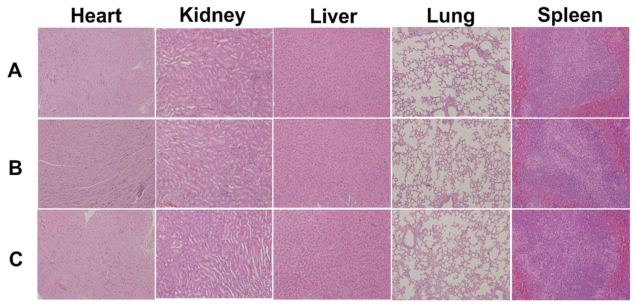

Fig. 10 Micrographs of H&E stained organ slices from (A) saline, before (B) and after (C) NIR laser treated groups.

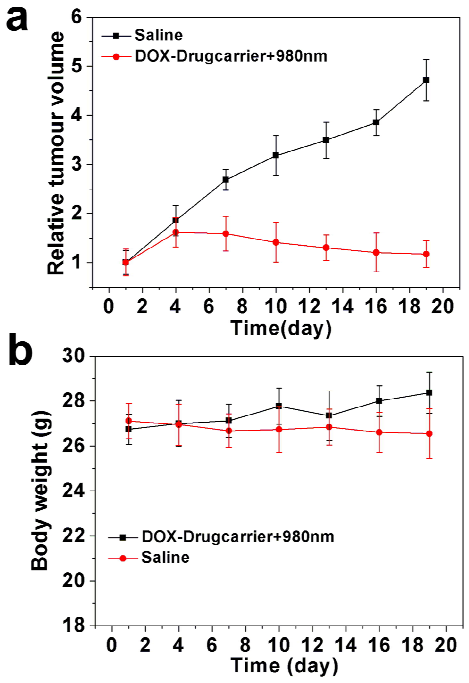

Fig. 11 (a) The tumour growth curve of different groups of mice after treatment (The tumour volumes were normalized to the initial sizes). (b) The body weight change curve of different groups of mice. The body weights were normalized to the initial ones.

Drug administration experiments were carried out on tumor-bearing nude mice to evaluate the NIR-controlled drug sustainable release in living tissue. Before that, systematic toxicity in *vivo* was verified to ensure the safety of our nanocarrier to the living issue. As shown in Fig. 10, there was no significant organ damage in the group of DOX-loaded without laser treatment compared to the saline group. The DOX-loaded nanocarrier (DOX-MUCNP@C18@PSMN-FA) was intratumorally injected into tumor-bearing mice at an interval of 2 days, followed by exposure of 980 nm irradiation (60 mW cm^{-2}) for 30 min each day for 19 d. The anti-tumor efficacy of NIR-triggered DOX release was investigated by the changes in tumor volume. Compared to the control groups, DOX-loaded drugcarrier inhibited tumor growth more efficiently with NIR laser treatment (Fig. 11a). The results demonstrated that by adoption NIR light as an excitation source, the light-controlled drug sustained release could be successfully realized in living tissue. And the mice weights results during the treatment period

(Fig. 11b) also suggested the safety of our nanocarrier and the effective treatment. At last, all mice were sacrificed and all organs and tumors were harvested. The histopathological examination results showed there was also no significant damage after the mice undergone the treatment period. And the results of tumors weight showed a significant and intuitive inhibitory effect with the treatment (Fig. S3).

Conclusion

In summary, we have prepared a NIR-responsive upconversion nanocomposites/polymer nanocarrier with good biocompatibility and active tumor targeting ability *via* a facile self-assembly strategy. Excited by 980 nm NIR light, the UCNP core emitted UV light which could trigger light-responsive amphiphilic copolymer shell uncaging the upconversion nanocomposites, resulting in the release of anticancer drugs (80 wt% in 24 h). In *vitro* experiments confirmed the biocompatibility, active tumor targeting ability and bioimaging ability of the nanocarrier. Both in *vitro* and in *vivo* studies confirmed the feasibility of NIR-triggered drug release and suggested a potential application of this multifunctional nanocarrier in biomedical field.

Acknowledgements

We gratefully acknowledge the financial support provided by National Natural Science Foundation of China (21336005, 21301125, 81302382), Natural Science Foundation of Jiangsu Province (BK2012625), Natural Science Foundation of the Jiangsu Higher Education Institutions of China (13KJB430022), Chinese-Singapore National Joint Project (2012DFG41900), Suzhou Nano-project (ZXG201420) and Joint Research Projects of SUN-WIN Joint Research Institute for Nanotechnology.

Notes and references

[a]*College of Chemistry, Chemical Engineering and Materials Science,Collaborative Innovation Center of Suzhou Nano Science and Technology, Soochow University, Suzhou, 215123 China.*
[b]*School of Radiation Medicine and Protection, Medical College of Soochow University, Suzhou, Jiangsu 215123, China*
[c] *State Key Laboratory of Treatments and Recycling for Organic Effluents by Adsorption in Petroleum and Chemical Industry, Suzhou, 215123 China.*
** E-mail: linajun@suda.edu.cn, lujm@suda.edu.cn; Tel./Fax: +86 (0) 512-6588 0367.*

†Electronic Supplementary Information (ESI) available: Experimental section. See DOI: 10.1039/b000000x/

1. (a) J. F. Gohy and Y. Zhao, *Chem. Soc. Rev*., 2013, **42**, 7117. (b) S. Mura, J. Nicolas and P. Couvreur, *Nature Materials*, 2013, **12**, 991. (c) E. G. Kelley, J. N. L. Albert, M. O. Sullivan and T. H. Epps, *Chem. Soc. Rev*., 2013, **42**, 7057. (d) F. D. Jochum and P. Theato, *Chem. Soc. Rev*., 2013, **42**, 7468. (e) J. Wu, N. Kamaly, J. J. Shi, L. L. Zhao, Z. Y. Xiao, G. Hollet, R. John, S. Ray, X. Y. Xu, X. Q. Zhang, P. W. Kantoff and O. C. Farokhzad, *Angew. Chem. Int. Ed*., 2014, **53**, 8975.
2. (a) S. Yang, N. J. Li, D. Y. Chen, X. X. Qi, Y. J. Xu, Y. Xu, Q. F. Xu and J. M. Lu, *J. Mater. Chem. B*,2013, **1**, 4628. (b) P. F. Gao, L. L. Zheng, L. J. Liang, X. X. Yang, Y. F. Li and C. Z. Huang, *J. Mater. Chem. B*, 2013, **1**, 3202. (c) K. Radhakrishnan, J. Tripathy and A. M. Raichur, *Chem. Commun*., 2013, **49**, 5390. (d) P. C. Du, H. Y. Yang, J. Zheng and P. Liu, *J. Mater. Chem. B*, 2013, **1**, 5298.
3. (a) C. Brieke, F. Rohrbach, A. Gottschalk, G. Mayer and A. Heckel, *Angew. Chem. Int. Ed.*, 2012, **51**, 2. (b) G. Pasparakis, T. Manouras, P. Argitis and M. Vamvakaki, *Macromol. Rapid. Commum.*, 2012, **33**, 183. (c) F. Ercole, T. P. Davis and R. A. Evans, *Polym. Chem.*, 2010, **1**, 37.
4. (a) X. Mei, S. Yang, D. Y. Chen, N. J. Li, H. Li, Q. F. Xu, J. F. Ge and J. M. Lu, *Chem. Commun*., 2012, **48**, 10010. (b) M. L. Viger, M. Grossman, N. Fomina and A. Almutairi, *Adv. Mater.*, 2013, **25**, 3733. (c) Y. Wang, C. Y. Hong and C. Y. Pan, *Biomacromolecules*, 2012, **13**, 2585. (d) C. Chen, L. Zhou, J. Geng, J. S. Ren and X. G. Qu, *Small*, 2013, **9**, 2793.
5. (a) R. X. Duan, F. Xia and L. Jiang, *ACS Nano*, 2013, **7**, 8344. (b) Y. H. Chien, Y. L. Chou, S. W. Wang, S. T. Huang, M. C. Liau, Y. J. Chao, C. H. Su and C. S. Yeh, *ACS Nano*, 2013, **7**, 8516. (c) K. C. Hribar, M. H. Lee, D. Lee and J. A. Burdick, *ACS Nano*, 2011, **5**, 2948.
6. (a) Y. Zhao, *Macromolecules*, 2012, **45**, 3647. (b) C. Q. Huang, Y. Wang, C. Y. Hong and C. Y. Pan, *Macromol. Rapid. Commun.*, 2011, **32**, 1174. (c) J. M. Schumers, O. Bertrand, C. A. Fustin and J. F. Gohy, *J. Polym. Sci., Part A: Polym. Chem.*, 2012, **50**, 599.
7. (a) J. Shen, G. Y. Chen, T. Y. Ohulchanskyy, S. J. Kesseli, S. Buchholz, Z. P. Li, P. N. Prasad and G. Han, *Small*, 2013, **9**, 3213. (b) S. Kumar, J. F. Allard, D. Morris, Y. L. Dory, M. Lepage and Y. Zhao, *J. Mater. Chem.*, 2012, **22**, 7252. (c) G. Liu, W. Liu and C. M. Dong, *Polym. Chem.*, 2013, **4**, 3431.
8. (a) J. N. Liu, W. B. Bu, L. M. Pan and J. L. Shi, *Angew. Chem. Int. Ed*., 2013, **52**, 1. (b) J. Cao, S. S. Huang, Y. Q. Chen, S. W. Li, X. Li, D. W. Deng, Z. Y. Qian, L. P. Tang and Y. Q. Gu, *Biomaterials*, 2013,**34**, 6272. (c) X. Zhang, P. P. Yang, Y. L. Dai, P. Ma, X. J. Li, Z. Y. Cheng, Z. Y. Hou, X. J. Kang, C. X. Li and J. Lin, *Adv. Funct. Mater.*, 2013, **23**, 4067. (d) K. Dong, Z. Liu, Z. H. Li, J. S. Ren and X. G. Qu, *Adv. Mater.*, 2013, **25**, 4452.
9. (a) Y. M. Yang, B. Velmurugan, X. G. Liu and B. G. Xing, *Small*, 2013, **9**, 2937. (b) J. Zhou, Z. Liu and F. Y. Li, *Chem. Soc. Rev*., 2012, **41**, 1323. (c) Y. M. Yang, Q. Shao, R. R. Deng, C. Wang, X. Teng, K. Cheng, Z. Cheng, L. Huang, Z. Liu, X. G. Liu and B. G. Xing, *Angew. Chem.*, 2012, **124**, 3179.
10. (a) L. Chen, C. Wang ang Z. Liu, *Nanoscale*, 2013, **5**, 23. (b) P. A. Ma, H. H. Xiao, X. X. Li, C. X. Li, Y. L. Dai, Z. Y. Cheng, X. B. Jing and J. Li, *Adv. Mater.*, 2013, **25**, 4898. (c) J. Zhu, Y. J. Lu, Y. G. Li, J. Jiang, L. Cheng, Z. Liu, L. Guo, Y. Pan and H. W. Gu, *Nanoscale*, 2014, **6**, 199.
11. Q. J. Xing, N. J. Li, D. Y. Chen, W. W. Sha, Y. Jiao, X. X. Qi, Q. F. Xu and J. M. Lu, *J. Mater. Chem. B*, 2014, **2**, 1182.
12. B. Yan, J. C. Boyer, N. R. Branda and Y. Zhao, *J. Am. Chem. Soc.*, 2011, **133**, 19714.
13. J. P. Yang, Y. H. Deng, Q. L. Wu, J. Zhou, H. F. Bao, Q. Li, F. Zhang, F. Y. Li, B. Tu and D. Y. Zhao, *Langmuir*, 2010, **26**, 8850.
14. W. D. Ji, N. J. Li, D. Y. Chen, X. X. Qi, W. W. Sha, Y. Jiao, Q. F. Xu and J. M. Lu, *J. Mater. Chem. B,*2013, **1**, 5942.